

DEVELOPMENT OF A GENERALIZED LINEAR SKULL FRACTURE CRITERION

Philemon Chan, Zi Lu and Paul Rigby

L-3/Jaycor

USA

Erik Takhounts

NHTSA

USA

Jiangyue Zhang, Narayan Yoganandan and Frank Pintar

Medical College of Wisconsin

USA

Paper Number 07-0227

ABSTRACT

This work develops a generalized linear skull fracture criterion, the skull fracture correlate, SFC, applicable to impacts by flat targets on the skull in any angle. The SFC is the averaged acceleration over the HIC15 time interval based on data obtained from Hybrid-III headform impact tests. For 15% or less probability of skull fracture the threshold is $SFC < 124$ g, with a 95% confidence band of $96 < SFC < 144$ g. The SFC correlation is established based on logistic regression against an extensive set of post mortem human specimen (PMHS) data. The biomechanical basis of SFC is validated by its good correlation with skull strain calculated using an anthropomorphic finite element model of the skull. This work is an extension and refinement of recent research results including the use of newly obtained PMHS data combined with historical data. Finite element model simulations were performed for all PMHS tests conducted for data comparison and statistical analysis.

INTRODUCTION

At present, in Europe, Japan, Australia, and the United States, a single Hybrid-III based Head Injury Criterion (HIC), is the standard for protection against generalized head injury in a frontal car crash. Current NCAP side impact crash tests use a side impact dummy (Part 572.F) with a Hybrid-III head/neck complex. Recently, biomechanically based multi-component criteria have been developed to separately protect against DAI, SDH, and brain contusions [Takhounts, et al., 2003]. The development of multi-mode injury criteria has the potential to advance the science of head protection.

Previous work by Hodgson and Thomas et al [1971 and 1973] has provided historical skull fracture data for various impact speeds, target compliances, and surface curvatures. In their tests, embalmed whole body Post Mortem Human Specimens (PMHS) were placed on a hinged pallet pivoted at the feet of the specimen, with the head extending over the edge. Known head weights varied between 3.2 and 5.4 kg with an average of 4.7 kg, which is close to the 4.5-kg weight of the 50th percentile male Hybrid-III headform. Impacts against flat targets, cylinders with large radius of curvature, and rubber targets produced primarily linear skull fracture while impact against rigid hemispheres and rigid cylindrical targets with small radius of curvature produced comminuted fracture. Impact speeds varied within $\pm 20\%$ of the theoretical free drop value with a standard deviation of 8%.

Recently, a considerable amount of new skull fracture data have been obtained by the Medical College of Wisconsin (MCW) under the sponsorship of the US National Highway Traffic Safety Administration (NHTSA) using unembalmed free head drops against targets similar to those used by Hodgson and Thomas, including cylindrical and flat targets. Compared to the hinged drop test method of Hodgson and Thomas, free drops of isolated head specimens would provide more accurate specification of impact conditions and allow for higher impact speeds. The softest target used by Hodgson and Thomas was durometer 60 (D60) neoprene. The new tests extended the target compliance to softer materials.

We have developed the linear skull fracture correlate (SFC) risk factor for skull fracture based on biomechanical understanding of the underlying injury

mechanism [Vander Vorst et al, 2003 and 2004]. In the case of the human skull, tensile strain in the compact tables is an indicator of fracture [Wood, 1971]. Skull fracture depends on both the geometry and compliance of the impacting target material and the weight of the head. Together, these factors determine the stress and strain distributions generated in the skull. Fracture occurs when the ultimate strain is exceeded. However, skull strain data at the location of fracture is difficult to measure in an impact test but it can be calculated with a finite element model (FEM) using the PMHS test conditions as input. Furthermore, it is desirable that a risk factor can be computed using data obtained from an anthropomorphic test device (ATD), such as the Hybrid-III headform.

Vander Vorst et al [2003] first developed the biomechanically-based linear skull fracture correlate for frontal impact using PMHS data mostly from Hodgson and Thomas [1971, 1973] and some recent data from the Medical College of Wisconsin for correlation with Hybrid-III headform tests and finite element model simulations. In this early work, FEM simulations were performed using an idealized spherical head model with a uniform skull layer of inner table, diploe and outer table. SFC was established as the averaged headform acceleration over the HIC time interval. The main finding from this first work was that the skull strain calculated from the FEM, the fracture data and SFC all correlated well with one another with well defined confidence bands, hence validating the biofidelity of SFC.

Further work was presented by [Vander Vorst et al, 2004] in expanding the validity of SFC to lateral impact using more newly obtained PMHS data. Different from the earlier work, the work presented in 2004 by Vander Vorst et al used an anthropomorphic FEM of the head with the calculated strain again showing good correlation with PMHS data and SFC. Since then, even more new PMHS data have been obtained that continue to validate the skull fracture data correlations with FEM-calculated strain and SFC. The significance of using the SFC is that it can be computed easily using data obtained from the Hybrid-III headform that can be implemented in standard tests.

The objective of this work is to develop a generalized linear skull fracture criterion for frontal and lateral impacts. The main effort is to refine and bolster the skull strain and SFC correlations with fracture data by pooling all the PMHS data together for analysis.

All frontal drop tests were simulated again using the same anthropomorphic FEM that was used for the lateral impact studies by [Vander Vorst et al, 2004]. The results will lead to skull fracture criteria that are based on the most comprehensive dataset known to date.

METHODS

Frontal impact test cases exhibiting primarily linear skull fracture were extracted from the Hodgson and Thomas [1971 and 1973] data set. Tests against slender rods and hemispheres were excluded since they resulted in depressed comminuted fractures instead of the linear fractures caused by the flat and 5-cm diameter cylindrical targets. Anomalous cases, as reported by Hodgson and Thomas, were also excluded. The analysis of the data from Hodgson and Thomas has been presented in detail previously by Vander Vorst et al [2003].

New lateral impact tests were conducted at the Medical College of Wisconsin using isolated PMHS head specimens. They are hereafter referred to as the MCW tests. A total of thirty-three unembalmed specimens free from HIV and Hepatitis B and C were tested. The intracranial contents were replaced with Sylgard Gel, except for four of the specimens which were left as is. The Institutional Review Board of the Medical College of Wisconsin approved the protocol. Pretest radiographs and computed tomography (CT) images of the specimens were obtained. Lateral impact tests were conducted by dropping the specimens against either flat or cylinder targets at velocities ranging from 2 to 10 m/s. Figure 1 shows a schematic diagram of the test set up. The inferior-superior axis of the specimen was situated at a 10-degree angle with respect to the target, and the anterior-posterior axis was parallel with the target. The orientation of the PMHS head for lateral impacts was such that the same anatomical point, at the temporo-parietal junction, would always be impacted. Because of individual anatomical differences, the skull had to be slightly tilted one way or the other by a few degrees to obtain the orientation. We chose a head alignment angle that is known to produce linear skull fractures that are representative of what occurs in the real world [Yoganandan et al, 1995]

Each specimen was impacted at increasing heights with a single impact at each height, and radiographs were obtained between drops. Impact force histories were recorded using a six-axis load cell. Signals were recorded using a digital data acquisition system (DTS

Technologies, Seal Beach, CA) at a sampling frequency of 12.5 kHz and filtered according to SAE Channel Class 1000 specifications [SAE, 1998]. Testing of a specimen was terminated when fracture was detected or the load cell limit was reached. The specimens underwent CT scanning after the final impact. Again, details of the analysis of the MCW data were previously presented by Vander Vorst et al [2004].

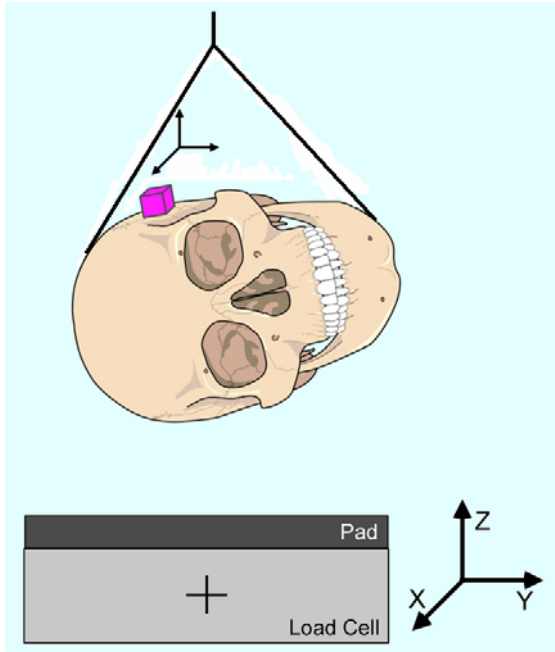


Figure 1. MCW test set up.

Drop tests using a 50th percentile male Hybrid-III headform were conducted corresponding to all PMHS test conditions for calculation of SFC [Vander Vorst et al, 2003 and 2004]. Three repeated drops were made for each impact condition. Repeated tests were checked for consistency and computed risk factors were averaged for statistical analysis. SFC is the averaged acceleration over the HIC time interval ΔT_{HIC}

$$SFC = \frac{\Delta V_{HIC}}{\Delta T_{HIC}} \quad (1)$$

where ΔV_{HIC} is the averaged velocity. For the present work the HIC15 time interval was used but due to the short impact duration (few milliseconds) involved the use of HIC36 time interval would not change the SFC results.

Simulations were carried out for all PMHS tests using the same anthropomorphic FEM presented by

[Vander Vorst et al., 2004]. All frontal drops that were previously simulated using the spherical model were simulated again using the anthropomorphic FEM. All new lateral drop tests performed since 2004 were also simulated. The model was composed of 24,000 elements resolving the outer and inner tables, diploe, brain, scalp, and face. The mass of the baseline model was 4.54 kg. The skull components were modeled using fully integrated thick shells and the brain, scalp, and face were modeled with fully integrated bricks. Since this model was based on CT imaging of a PMHS, the skull shape and thickness are anatomically correct. The thickness of the compact skull tables was set to be 1.3 mm uniformly, as they were too thin to be resolved from the CT scan. The 1.3-mm value was based on measurements of photographic cross-sections from the Visible Man project [National Library of Medicine, 2000]. The properties of the biological materials were taken from the open literature and previously presented [Vander Vorst et al., 2003]. All finite element model simulations were performed using Version 9.70 of LS-Dyna3d software [Livermore Software Technology Corporation, 2003].

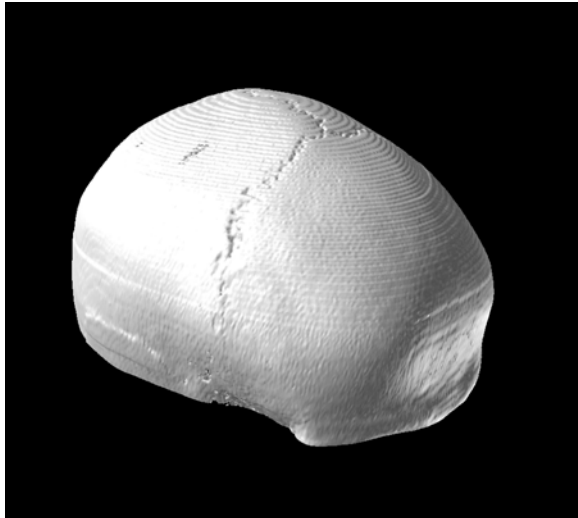
For each PMHS drop test, the SFC calculated from the corresponding Hybrid-III test and the peak skull tensile strain from the inner and outer tables calculated from the finite element model along with the fracture outcomes of the test were placed in a database for statistical analysis. To account for varying head weights, SFC was normalized by the factor $MH/4.54$ kg, where MH is the actual mass of the test specimen in kg [Vander Vorst et al., 2003]. The data were analyzed by logistic regression [Hosmer and Lemeshow, 1989] using the longitudinal, population-averaged model with presumed failures [Zeger and Lian, 1986; Chan et al., 2001]. The data were treated as longitudinal since each specimen proceeded through a test matrix from low to high drop heights with repeated testing. Hence, the specimen responses were not independent between tests. When a specimen fractured at a given drop height, it was presumed to fail at all higher drop heights. All statistical computations were carried out using the STATA software [Stata, 1999].

Statistical analysis was carried out by pooling the PMHS data from the Hodgson and Thomas and MCW tests together. Analysis of the fracture outcomes and FEM results were carried out to evaluate the differences between impacts against cylindrical and flat targets for frontal and lateral drops. As will be presented later, the generalized linear fracture correlations with SFC and skull strain

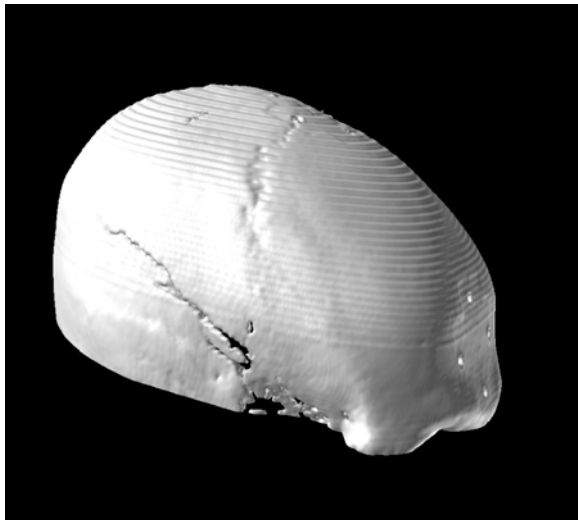
were established by using only the data obtained from the flat target tests.

RESULTS

The Hodgson and Thomas [1971 and 1973] tests contributed all the frontal drop data and some lateral drop data used for the present work. The MCW tests contributed the majority of the lateral drop data. Figure 2 shows an example of the three-dimensional reconstruction of the CT data before and after a test that resulted in fracture as performed by MCW.



(a) Pretest scan



(b) Posttest scan showing fracture

Figure 2. Reconstruction of CT scans.

Frontal vs. Lateral PMHS Skull Fracture

Analysis of the selected outcomes obtained from tests conducted at the same drop height against the same target material suggests that frontal drops are more likely to cause fracture than lateral drops (Figure 3). For the D90 cylindrical target, a 48-in drop height resulted in 100% fracture for frontal impact vs. only 50% for lateral impact, and it needed 72-in drop height for the lateral impact to result in 100% fracture (Figure 3a). For the D90 flat target, the frontal impact resulted in 100% fracture at 36-in drop height while the lateral impact resulted only in 33%, and it also needed 72-in drop height for the lateral impact to result in 100% fracture (Figure 3b). For the drops against the rigid flat target, 100% fracture was observed for the frontal impact at 10-in drop height while only 45% was observed for the lateral impact, and it needed 15-in drop height for the lateral impact to produce 100% fracture (Figure 3c). For the drop outcomes against D90 cylindrical and flat targets shown in Figures 3a and b, respectively, the data for frontal drops are from Hodgson and Thomas while the data for lateral drops are from MCW, while the rigid target data shown in Figure 3c are solely from Hodgson and Thomas.

Based on their own PMHS test results, Hodgson and Thomas had commented that “The head is strongest in respect to fracture in the rear, side and front in that order” [Hodgson and Thomas et al, 1971]. Because of biological variability for PMHS tests, logistic regression was performed to fully determine the difference between the frontal and lateral skull fracture resistance by pooling all the data together with confidence band determined. Statistical correlations of the pooled dataset with FEM results and SFC were established as will be presented.

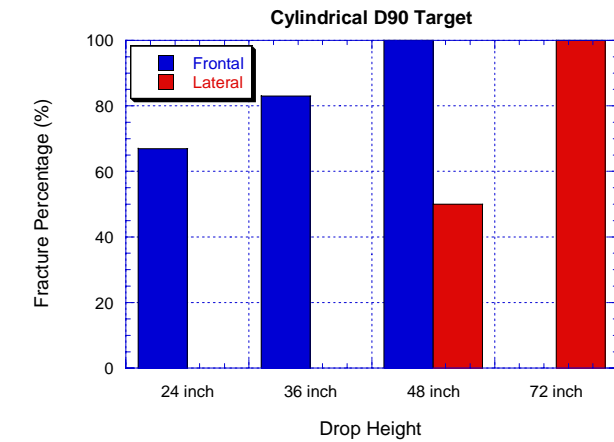
FEM Skull Strain

The pattern of the outer table skull strain calculated from the FEM shows a peak compressive (negative) strain occurring at the impact site with the tensile (positive) strain peaking nearby but away from the impact site as illustrated in Figure 4. This pattern holds true for frontal as well as lateral impacts against cylindrical and flat targets over the full range of target compliance tested. The contact between the head and target creates a large concentrated compression at the contact point (blue) while the skull bending creates large tensile strains in a nearby region (red) as expected from the perspective of bending mechanism (Figures 4a-d).

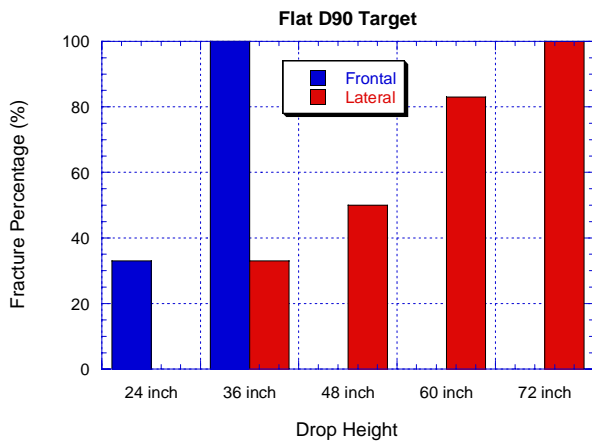
For comparison, the corresponding principal strain patterns in the inner table are shown in Figure 5. Compared to the outer table (Figure 4), the compressive (negative) strains in the inner table are one to two orders of magnitude smaller and they occur around the rim of the inner table (Figure 5). The location of the peak tensile strain in the inner table is not too far from that in the outer table (Figures 4-5). We use the maximum tensile strain from the inner and outer table as indicator for skull fracture and data correlations. For the case shown in Figures 4c and 5c, the location of the peak skull tensile strain (red) in the outer and inner table as calculated from the finite element model occurs in close proximity to the location of the observed fracture (Figure 2b), which is consistent with the skull fracture mechanism proposed by [Wood, 1971].

Skull Fracture Correlations

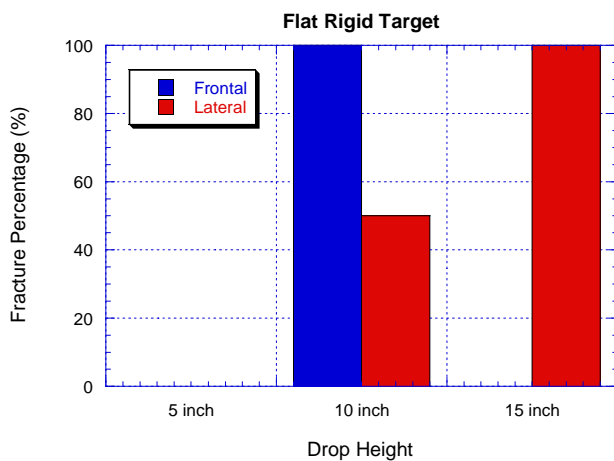
Logistic regression of the combined dataset suggest the frontal drops will have a higher risk of fracture than the lateral drops, and both frontal and lateral correlations have good confidence bands (Figures 6a-b). Based on the mean correlation, a skull strain of 0.2 would result in 52% of fracture for frontal drops but only 13% for lateral drops (Figures 6a-b). This seems to be consistent with the trend of fracture outcomes shown in Figure 3. Nonetheless, a strain-fracture correlation with a fairly good confidence band can be obtained for the combined frontal and lateral drop dataset (Figure 6c). The SFC correlation with fracture data also shows a similar trend as the strain correlation (Figure 7). Figures 7a-b suggest frontal drops would result in a higher probability of fracture than lateral drops. Again, a combined SFC correlation with fracture can still be obtained with a good confidence band (Figure 7c).



(a) D90 neoprene cylindrical target

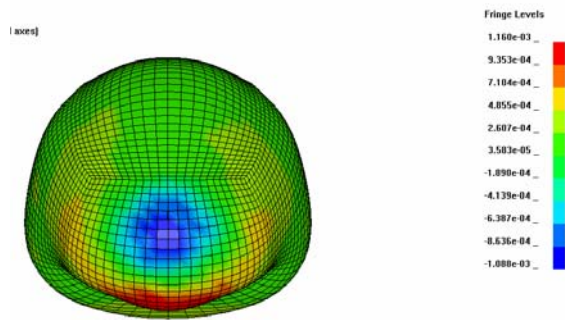


(b) D90 neoprene flat target

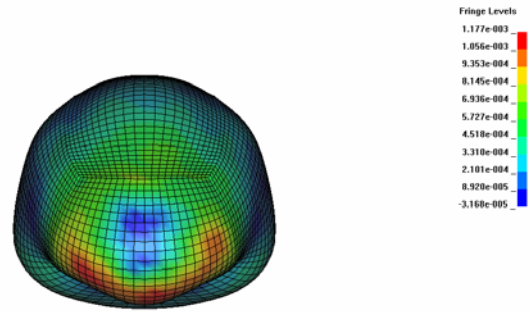


(c) Rigid flat target

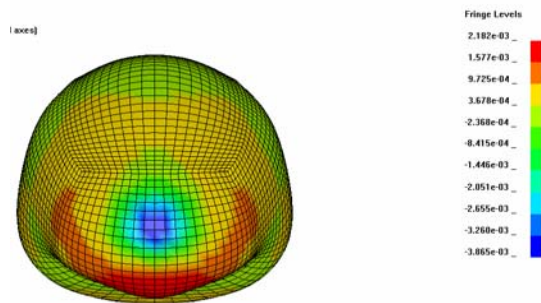
Figure 3 Skull fracture data comparison.



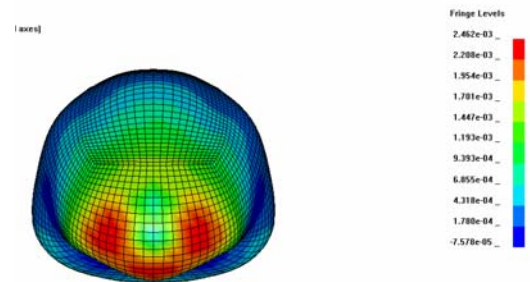
(a) Frontal impact, D40 flat target



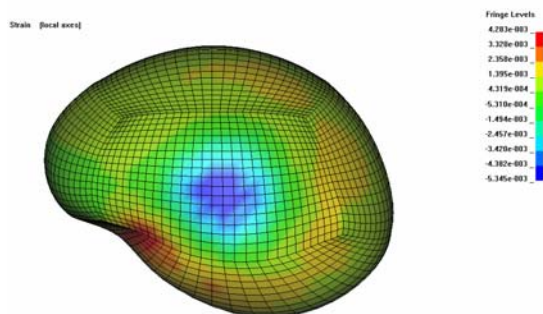
(a) Frontal impact, D40 flat target



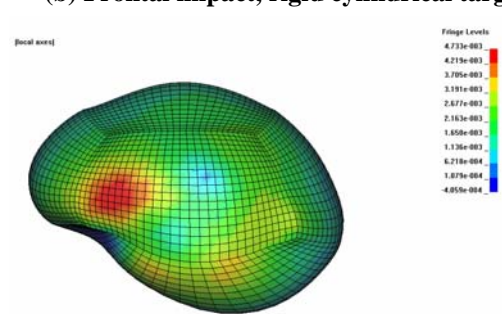
(b) Frontal impact, rigid cylinder target



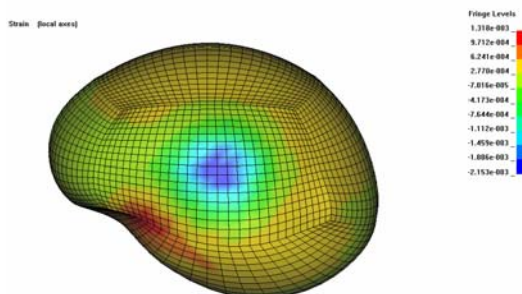
(b) Frontal impact, rigid cylindrical target



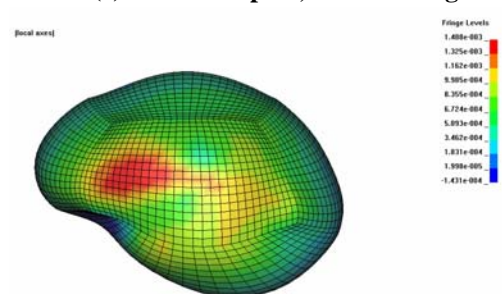
(c) Lateral impact, D90 flat target



(c) Lateral impact, D90 flat target



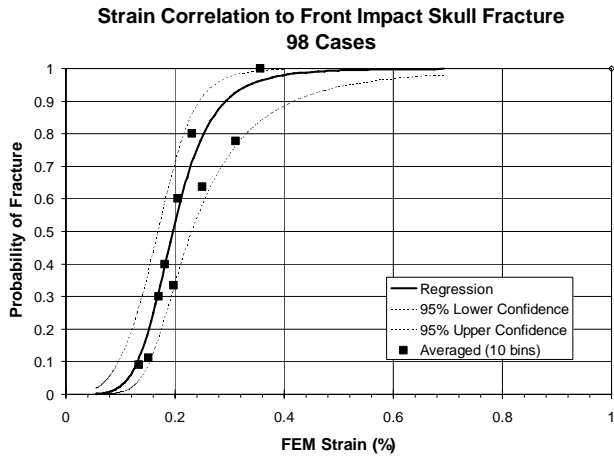
(d) Lateral impact, rigid cylinder target



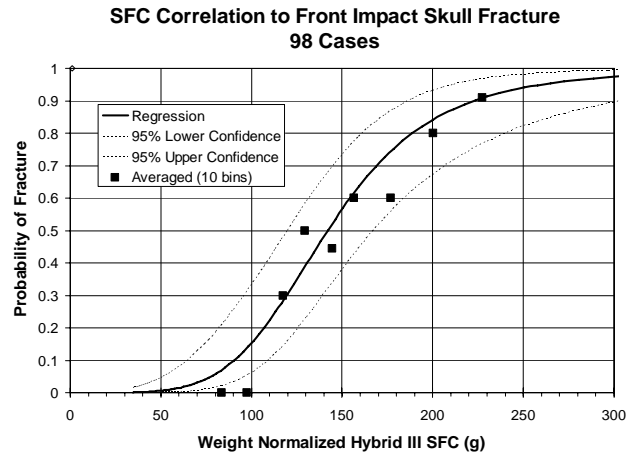
(d) Lateral impact, rigid cylindrical target

Figure 4. Principal strain in outer table.

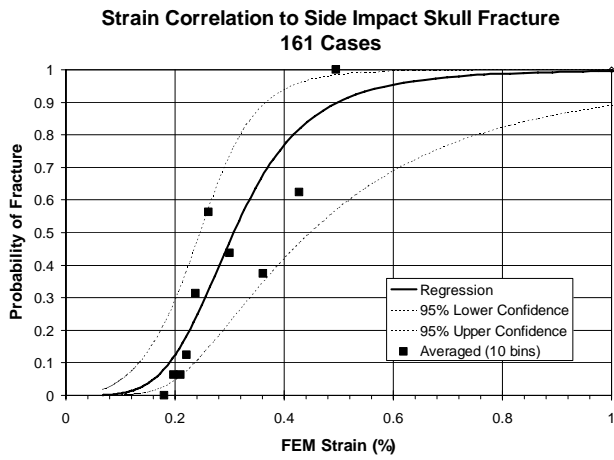
Figure 5. Principal strain in inner table.



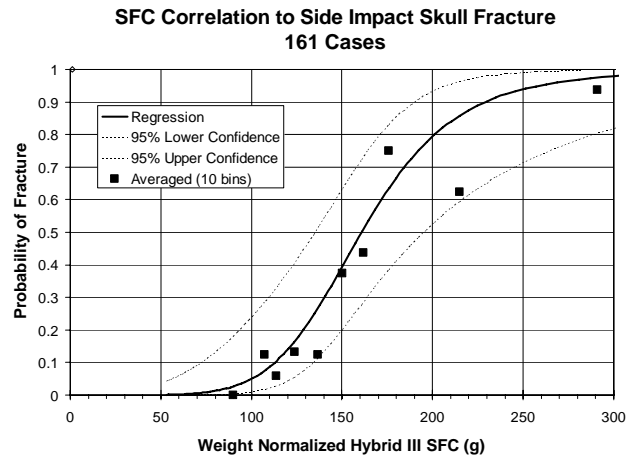
(a) Frontal drop



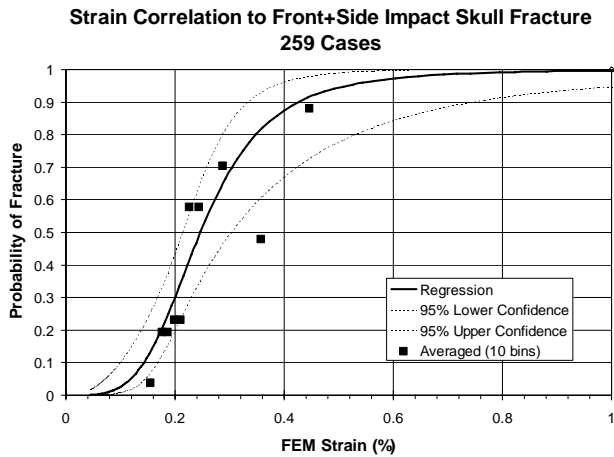
(a) Frontal drop



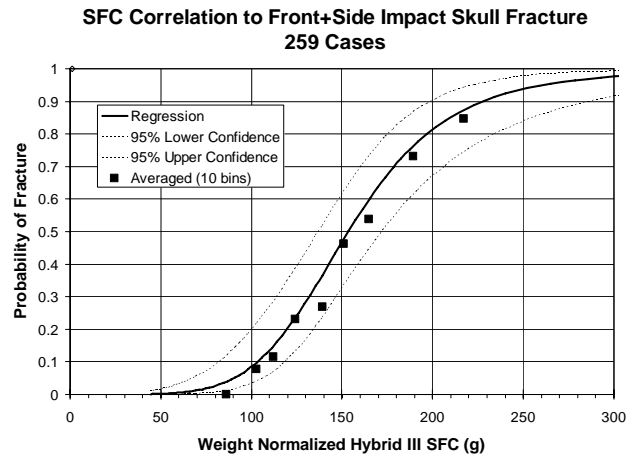
(b) Lateral drop



(b) Lateral drop



(c) Combined frontal and lateral correlation



(c) Combined frontal and lateral correlation

Figure 6. Strain correlation with skull fracture data for all tests.

Figure 7. SFC correlation with skull fracture data for all tests.

The SFC correlation with strain suggests that there is a different fracture trend between the impacts against cylindrical and flat targets. Figure 8 shows that a good linear correlation between SFC and strain is established, especially when only the data for the flat plate target tests are considered. As shown in Figure 8, the data from the cylindrical target tests for both frontal and lateral drops deviate from the linear correlation for the flat target data quite significantly. If only the data for the flat plate targets are used, SFC correlates well with strain with the coefficient of R^2 of 0.95 (Fig. 8).

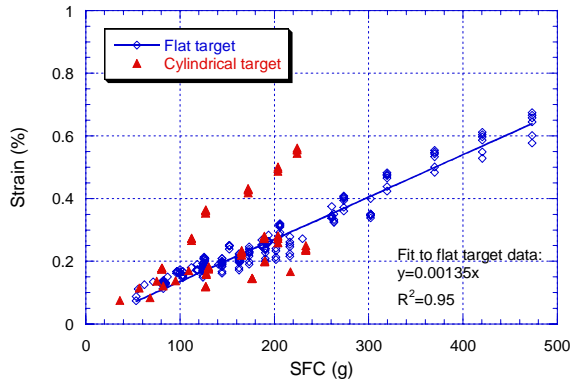


Figure 8. SFC correlation with strain.

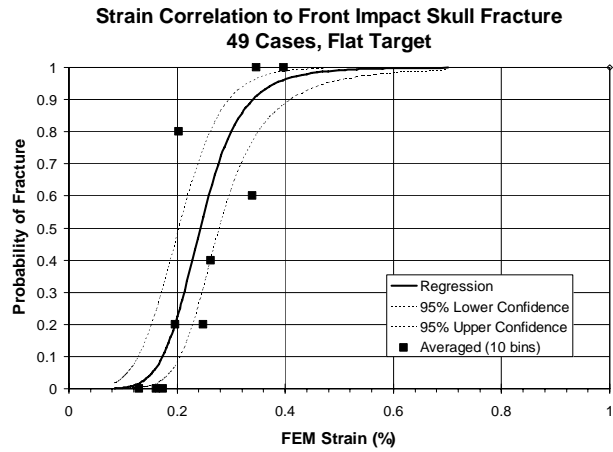
Therefore, to establish a generalized correlation for linear fracture, we only used the flat target test data (Figure 9). Based on the flat target data, Figures 9a-b show that the strain-fracture correlations for the frontal and lateral drops are quite close to each other with the frontal correlation slightly higher than the lateral one, but the confidence band for the lateral correlation is wider. The strain-fracture correlation for the frontal impact is

$$\ln\left(\frac{P}{1-P}\right) = 6.51 * \ln(strain) + 9.21 \quad (2)$$

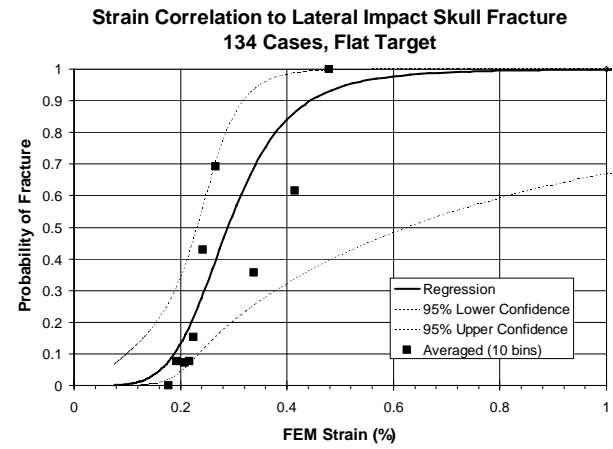
and for lateral impact,

$$\ln\left(\frac{P}{1-P}\right) = 5.12 * \ln(strain) + 6.36 \quad (3)$$

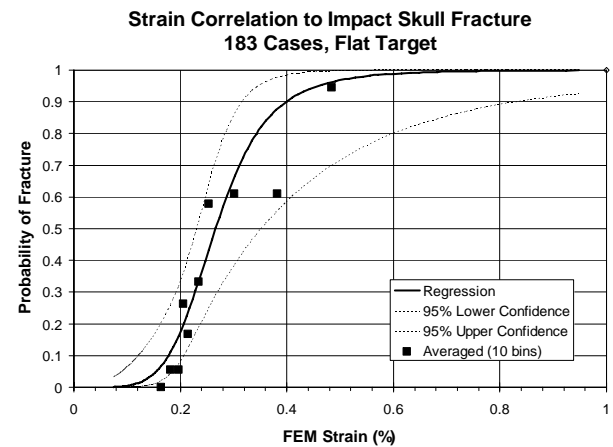
where P is the probability of fracture. The strain of 0.2% corresponds to 22% mean probability of fracture for frontal impact vs. 13% for lateral impact (Eq. 2 vs. 3 and Figure 9a vs. 9b). The difference in



(a) Frontal impact



(b) Lateral impact



(c) Frontal and lateral data combined

Figure 9. Skull strain correlation with fracture data for flat targets.

the strain-fracture correlation between frontal and lateral drops is small in terms of statistics, namely, the frontal correlation falls within the 95% confidence band of the lateral correlation (Figures 9a and b).

A generalized correlation with a good confidence band is obtained by combining the frontal and lateral drop data for the flat targets (Figure 9c). The generalized strain-fracture correlation for both frontal and lateral impacts is

$$\ln\left(\frac{P}{1-P}\right) = 5.43 * \ln(\text{strain}) + 7.19 \quad (4)$$

The strain of 0.2% corresponds to 18% mean probability of fracture.

Using only the flat target data, the SFC correlations with fracture are shown in Figure 10. For frontal impact, the SFC correlation is

$$\ln\left(\frac{P}{1-P}\right) = 8.98 * \ln(SFC) - 45.32 \quad (5)$$

and for lateral impact,

$$\ln\left(\frac{P}{1-P}\right) = 5.76 * \ln(SFC) - 29.59 \quad (6)$$

The mean SFC correlations also show frontal impacts giving slightly higher risk of skull fracture (Figure 10a vs. 10b) consistent with the strain-fracture correlations (Figure 9a vs. 9b). SFC of 150 g corresponds to 42% mean probability of fracture for frontal impact vs. 33% for lateral impact (Eq. 5 vs. 6 and Figure 10a vs. 10b).

It should also be noted that the difference in the SFC-fracture correlations between frontal and lateral drops against flat targets is small in terms of statistics as it can be seen that their 95% confidence bands overlap each other (Figures 10a-b). Combining the frontal and lateral data together, a generalized SFC correlation for linear skull fracture becomes

$$\ln\left(\frac{P}{1-P}\right) = 6.39 * \ln(SFC) - 32.53 \quad (7)$$

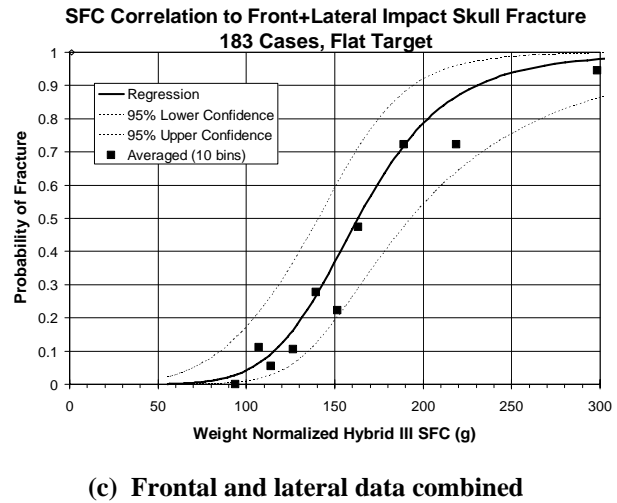
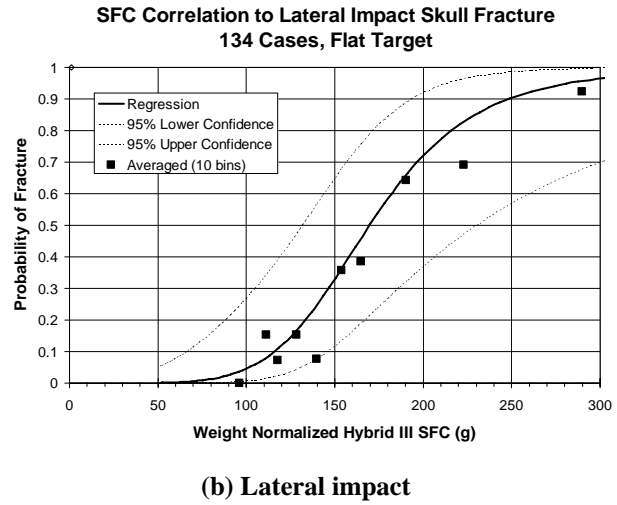
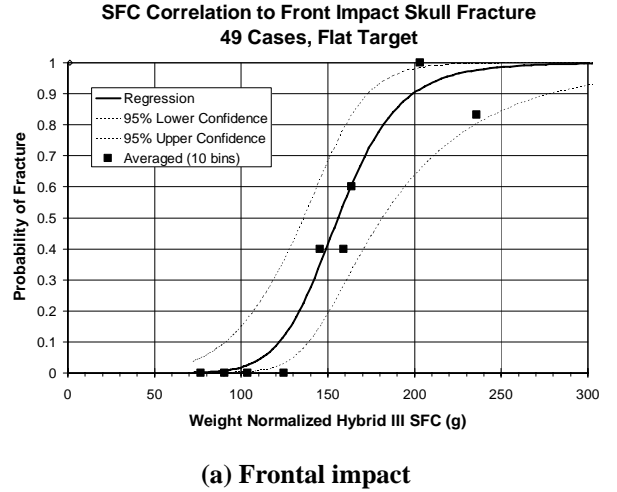


Figure 10. SFC correlation with fracture data for flat targets.

The confidence band of the generalized SFC regression is well behaved (Figure 10c). The SFC of 150 g corresponds to 37% mean probability of fracture. The 15% probability of generalized skull fracture, SFC_{15} , occurs at

$$SFC_{15} = 124\text{g} \quad (8)$$

with a 95% confidence band of (Figure 10c)

$$96 < SFC_{15} < 144\text{g} \quad (9)$$

It should be mentioned that the generalized SFC_{15} of 124g is slightly higher than the previously reported value of 120 g [Vander Vorst et al, 2004], while the new 95% confidence band can be considered comparable to the previous result of $73 < SFC_{15} < 149\text{g}$ for lateral impact and $96 < SFC_{15} < 133\text{g}$ for frontal impact.

DISCUSSION

By pooling the flat target data from frontal and lateral drops together, a generalized SFC is established (Eq. 7), and its biofidelity is validated against peak skull tensile strain calculated using the FEM. This generalized SFC is very close to the separate frontal and lateral impact correlations, with all 95% confidence bands overlapping each other (Figure 10). The use of the generalized SFC should be adequate since in real impact situations, it is impossible to determine or predict the impact angle accurately. The refined generalized SFC threshold for 15% mean probability of fracture is 124 g, which is very close to the previously estimated value of 120 g. The present result is based on correlation with over 30% more PMHS data samples than before.

The main reason why SFC correlates well with skull fracture data is that the effects of target compliance and contact area are well captured by SFC. Details of those findings have been previously presented [Vander Vorst et al, 2003, 2004]. In contrast, previous findings have shown HIC correlates poorly with skull fracture data because the target compliance and contact area effects are not well captured by HIC [Vander Vorst et al, 2003, 2004].

The hard nature of the cylindrical targets used for the PMHS tests may have exaggerated the difference in fracture risk between frontal and lateral drops. Note that the cylindrical targets used for the frontal and lateral drops were of D90 and rigid nature. The full range of target compliance was not used for the tests

with cylindrical targets. More future work is recommended to determine when focal or comminuted fracture begins, or when linear fracture does not apply.

The use of finite element model simulations will play a key role in improving the generalized skull fracture criteria because the injury mechanism can be studied rigorously using the model. Only through its good correlation with the FEM peak skull strain, can we establish the biomechanical basis of SFC. However, the peak skull strain may still not be the best risk factor that can be derived from the FEM simulations. We hypothesize that an improved risk factor that is more fracture mechanics-based than just the peak tensile strain can be developed using the FEM that will truly bring the frontal and lateral fracture correlations together, including the incorporation of the cylindrical target data. It is foreseeable that the generalized skull fracture criterion should be FEM-based. To accomplish that thin-film instrumentation placed on the headform is needed to measure the skull surface pressure distribution as input to the FEM for fracture prediction without the need for modeling the impacting target.

For the present work, the effects of biological variability on the correlations are probably still not fully captured. FEM simulations were not carried out using specimen-specific models, and only the 50th percentile Hybrid-III headform was used to collect data for all the PMHS drop tests. It is known that there is considerable variation in the skull thickness between head specimens, and it will also require much higher computational resolution to resolve these details that are actually very important for fracture predictions. Specimen mass was matched between the test specimen, the FEM, and SFC. Mass scaling may be inadequate for resolving geometrical and structural details. These effects are recognized as part of the limitations of the present work. It will be valuable to construct specimen-specific FEMs for simulation with comparison to the actual fracture data outcome. The FEM used did not involve a fracture material model. The present work is still mostly based on statistical correlation of FEM results with ATD and PMHS test outcomes with limited detailed comparison of simulation results with posttest CT data.

Another limitation of this work is that the generalized criteria developed were validated against flat target impact-induced, linear skull fracture data. Other fracture types, such as focal fractures, were not considered. It is worth mentioning that a fairly large

dataset, perhaps the most extensive to date with over 183 drops, has been used to establish the generalized skull fracture correlations.

CONCLUSION

A generalized injury criterion SFC, the average acceleration over the HIC time interval, is established for the flat target impact-induced, linear skull fracture for crashworthiness assessment. Its biomechanical basis is demonstrated by its good correlation with the skull strain regardless of impact locations or various target compliances. The criterion that the probability of skull fracture is less than 15% is $SFC_{15} < 124$ g.

ACKNOWLEDGMENTS

This research effort was sponsored by the National Highway Traffic Safety Administration, US Department of Transportation through a Joint Cooperative Research Agreement with the US Army Medical Research and Materiel Command under contract W81XWH-06-C-0051.

REFERENCES

Bandak, F.A. and Eppinger, R.H. 1994. "A Three-Dimensional Finite Element Analysis of the Human Brain under Combined Rotational and Translational Accelerations," SAE paper 942215, 38th Stapp Car Crash Proceedings, p. 279

Bandak, F.A. and Vander Vorst, M.J., Stuhmiller, L.M., Mlakar, P.F., Chilton, W.E., and Stuhmiller, J.H. 1995. "An Imaging-Based Computational and Experimental Study of Skull Fracture: Finite Element Model Development," *J. Neurotrauma*, 12(4): 679-688.

Chan, P.C., Ho., K.H., Kan, K.K., and Stuhmiller, J.H. 2001. "Evaluation of Impulse Noise Criteria Using Human Volunteer Data," *Journal of the Acoustical Society of America*, 110(4): 1967-1975.

Hodgson, V.R. and Thomas, L.M. 1971. "Breaking Strength of the Skull vs. Impact Surface Curvature," DOT HS-800 583, Contract No. FH-11-7609, Final Report.

Hodgson, Voigt R. and Thomas, L. Murray. 1973. "Breaking Strength of the Human Skull vs. Impact Surface Curvature," Report DOT HS-801002, National Technical Information Service, Springfield, Virginia.

Hosmer, D. and Lemeshow, S. *Applied Logistic Regression*, John Wiley & Sons, New York; 1989.
Johnson, K.L. (1985), *Contact Mechanics*, Cambridge University Press, London.

Livermore Software Technology Corporation, *LS-Dyna3d Users Manual*, 1998. Livermore, CA, 2003.
S.A.E. "Instrumentation for Impact Test – Part 1- Electronic Instrumentation," *Surface Vehicle Information Report*, Society for Automotive Engineers, Warrendale, Pa, J211-1; 1998.

Stata Users Guide. 1999, Stata Press, College Station, TX, 1999.

Takhounts, E., Eppinger, R., Campbell, J.Q., Tannous, R., Power, E. and Shook, L. 2003. "On the Development of the SIMon Finite Element Head Model," *Stapp Car Crash Journal*, Volume 47.

US Code of Federal Regulations, Title 49 (Transportation), Part 571 (Federal Motor Vehicle Safety Standards); 2003.

Vander Vorst, M., Stuhmiller, J., Ho, K., Yoganandan, N. and Pintar, F. 2003. "Statistically and Biomechanically Based Criterion for Impact-Induced Skull Fracture," 47th Annual Proceedings of the Association for the Advancement of Automotive Medicine, Lisbon, Portugal.

Vander Vorst, M. and Chan, P. C. 2004. "A New Biomechanically-based Criterion for Lateral Skull Fracture," 48th Annual Proceedings of the Association for the Advancement of Automotive Medicine.

Visible Human Project, National Library of Medicine, National Instituted of Health, Bethesda, Maryland, 2000.

Wood, J. L. 1971. "Dynamic Response of Human Cranial Bone," *J. Biomech.* 4: 1-12.

Yoganandan, N, Pintar, F. A., Sances, A Jr, Walsh P. R., Ewing, C. L., Thomas, D. J., Snyder, R. G. 1995. "Biomechanics of Skull Fracture," *J. Neurotrauma*: 12(4) pp.659-668, 1995.

Zeger, S.L. and Liang, K. 1986. "Longitudinal Data Analysis for Discrete and Continuous Outcomes," *Biometrics* 42, 121-130.